Chemical Geology 597 (2022) 120815

Contents lists available at ScienceDirect

Chemical Geology

journal homepage: www.elsevier.com/locate/chemgeo

Revised astronomically calibrated $^{40}Ar/^{39}Ar$ ages for the Fish Canyon Tuff sanidine – Closing the interlaboratory gap

D. Phillips [a,*], E.L. Matchan [a], H. Dalton [a], K.F. Kuiper [b]

[a] School of Geography, Earth and Atmospheric Sciences, The University of Melbourne, Parkville, VIC 3010, Australia
[b] Faculty of Earth and Life Sciences, Vrije Universiteit Amsterdam, the Netherlands

ARTICLE INFO

Editor: Balz Kamber

Keywords:
$^{40}Ar/^{39}Ar$ geochronology
Reference minerals
Fish Canyon Tuff
Alder Creek Rhyolite
Mount Dromedary

ABSTRACT

The $^{40}Ar/^{39}Ar$ geochronology method is capable of high precision (<0.05%), but remains limited by relatively large uncertainties in ^{40}K decay constants and the ages of natural reference mineral standards. The most widely used $^{40}Ar/^{39}Ar$ reference mineral is the well-known ca. 28 Ma Fish Canyon Tuff sanidine (FCTs). Several studies have attempted to calibrate FCTs against astronomically tuned tephra in Crete (Faneromeni A1 tephra) and Morocco (Messâdit Mes4 tuff) as well as deep-sea sedimentary sequences. Previously reported astronomically tuned ages range from 28.126 ± 0.019 to 28.21 ± 0.18 Ma (2σ), a range of ~0.3%, compared to precision levels of <0.05% achievable by new generation, multi-collector mass spectrometer systems. In this study, we revisit the astronomical calibration of FCTs. Relative to ages of 6.943 ± 0.005 Ma for A1 tuff sanidine (A1Ts) and 6.791 ± 0.010 Ma (2σ) for Mes4 tuff sanidine (Mes4Ts), we calculate revised astronomically tuned ages for Fish Canyon Tuff sanidine of 28.175 ± 0.012 Ma (±0.023 Ma, including the uncertainty in the age of A1Ts) and 28.176 ± 0.010 Ma (±0.042 Ma, including the uncertainty in the age of Mes4Ts), respectively (assuming negligible differential ^{39}Ar recoil loss). This age is within uncertainty of most recent astronomical intercalibrations, permitting calculation of inter-laboratory mean ages of 28.176 ± 0.010 (±0.023) Ma and 28.179 ± 0.009 (±0.042) Ma, respectively. As the astronomical age of the A1 tuff is more precise than that of the Mes4 tuff, we recommend that the former value is adopted as the astronomical age for FCTs. This age is consistent with available U-Pb zircon age data, but remains distinctly older than recent astronomical ages of 28.10 and 28.150 Ma inferred from deep-sea Ocean Drilling Program sediments, indicating that further work is required to align the astronomical tuning of terrestrial versus deep-sea sediments. Based on previous R-values for the Alder Creek Rhyolite sanidine (ACRs) and Mount Dromedary biotite (MD-2b) reference minerals, co-irradiated with FCTs, we calculate revised astronomically calibrated ages of 1.18342 ± 0.00069 (±0.009) Ma for ACRs and 99.323 ± 0.077 (±0.33) Ma for MD-2b, the latter amended to 99.20 ± 0.01 (±0.38) Ma to account for relative recoil loss of $^{39}Ar_K$. To further enhance the accuracy of $^{40}Ar/^{39}Ar$ ages, our study also highlights the need to carefully control neutron fluence gradients and consider recoil effects.

1. Introduction

The $^{40}Ar/^{39}Ar$ dating technique is a variation on the conventional K-Ar method and is based on the natural decay of ^{40}K to ^{40}Ar, where ^{39}Ar is produced by fast neutron irradiation (see Schaen et al., 2021 and references therein). The proportion of $^{39}Ar_K$ produced during irradiation is determined indirectly by co-irradiating reference minerals (also termed fluence monitors) of known age. Because argon isotopic ratios are measured, $^{40}Ar/^{39}Ar$ ages can be determined very precisely, with new generation mass spectrometers capable of precision levels <0.05% (e.g., Phillips and Matchan, 2013; Phillips et al., 2017; Phillips and Matchan, 2020; Phillips et al., 2020).

Despite the broad applicability of the $^{40}Ar/^{39}Ar$ technique to a range of K-bearing minerals across much of Earth history, the accuracy of the method remains limited by relatively large uncertainties in the potassium decay constants and the ages of key reference minerals (see Schaen et al., 2021 and references therein). Recent efforts to address these issues have included optimization of the $^{40}Ar/^{39}Ar$ method relative to the U-Pb technique (Renne et al., 2010, 2011) and calibration of reference minerals (e.g., Fish Canyon Tuff sanidine) to the astronomical timescale (e.

* Corresponding author.
E-mail address: dphillip@unimelb.edu.au (D. Phillips).

https://doi.org/10.1016/j.chemgeo.2022.120815
Received 26 October 2021; Received in revised form 14 March 2022; Accepted 15 March 2022
Available online 18 March 2022

g., Kuiper et al., 2004, 2008; Rivera et al., 2011, 2013; Phillips et al., 2017; Phillips et al., 2020; Niespolo et al., 2017). The optimization approach of Renne et al. (2010, 2011) appears to produce $^{40}Ar/^{39}Ar$ ages for Cenozoic samples that are slightly older than generally accepted ages and may require further refinement (see Phillips et al., 2017).

Two indirect approaches have been used to calibrate common $^{40}Ar/^{39}Ar$ reference mineral ages to the astronomical timescale, as their host units have not been identified in deep-sea sequences. The first approach involves calibration relative to astronomically tuned deep-sea cores that contain well-defined geological markers (e.g. Danish Ash-17; Knox, 1984) and/or geomagnetic polarity excursions, for which $^{40}Ar/^{39}Ar$ data are also available (e.g., Westerhold et al., 2015; Channell et al., 2020). The second approach involves $^{40}Ar/^{39}Ar$ analyses of reference minerals (e.g., Fish Canyon Tuff sanidine - FCTs) relative to tuff layers interbedded within astronomically tuned, terrestrial marine successions in the Mediterranean region, notably the A1 Tephra (A1T) in the Faneromeni section of Crete (Kuiper et al., 2004; Rivera et al., 2011, 2013; Phillips et al., 2017; Niespolo et al., 2017) and the Mes4 tuff in the Messâdit section, Morocco (Kuiper et al., 2008; Niespolo et al., 2017). In this study, we employ the latter approach and revisit the astronomical calibration of the age for the well-known Fish Canyon Tuff sanidine reference mineral.

The ca. 28 Ma, Fish Canyon Tuff sanidine (FCTs) (Cebula et al., 1986) is the most widely used $^{40}Ar/^{39}Ar$ reference mineral, due to its high potassium content, low atmospheric contamination levels and superior $^{40}Ar^*/^{39}Ar$ data reproducibility (e.g., Renne et al., 1998; Phillips et al., 2017). However, reported K-Ar and $^{40}Ar/^{39}Ar$ ages for FCTs vary from 27.54 ± 0.29 Ma to 28.39 ± 0.19 Ma (2σ), a spread of ~3% (e.g., Cebula et al., 1986; Renne et al., 1998, 2010, 2011; Lanphere and Baadsgaard, 2001; Spell and McDougall, 2003; Kuiper et al., 2008; Ganerød et al., 2011; Rivera et al., 2011; Hall, 2013; Niespolo et al., 2017; Phillips et al., 2017). Astronomically calibrated ages for FCTs relative to Mediterranean tuffs (A1T, Mes4) show a more restricted age range (28.126 ± 0.019–28.21 ± 0.18 Ma; 2σ; Kuiper et al., 2004, 2008; Phillips et al., 2017), but still vary by ~0.3%, which is well above current analytical precision capability (Table 1).

The above FCTs ages are mostly older than values estimated relative to astronomically tuned ash beds and/or geomagnetic excursions identified in Ocean Drilling Program (ODP) cores, which range from ~27.89–28.15 Ma (see Westerhold et al., 2015; Channell et al., 2020). For example, Westerhold et al. (2015) calculated an age for FCTs of 28.10 Ma, based on $^{40}Ar/^{39}Ar$ results for Ash-17 sanidine co-irradiated with FCTs (Storey et al., 2007). By correlating astronomical and $^{40}Ar/^{39}Ar$ ages for 16 geomagnetic excursions, Channell et al. (2020) estimated an FTCs age of 28.15 Ma.

Table 1
Previously reported R-values and $^{40}Ar/^{39}Ar$ ages for Fish Canyon Tuff sanidine (FCTs) relative to the ages of the A1 Tephra sanidine (A1Ts) and Mes4 Tuff sanidine (Mes4Ts).

R-value[1,2]	±2σ (abs.)	±2σ (%)	FCTs age (Ma)	±2σ (abs.)	±2σ (%)	Reference
$R_{FCTs/A1Ts}$[1]						
4.0888	0.0239	0.58	28.224	0.165	0.58	Kuiper et al. (2004)
4.0813	0.0026	0.06	28.172	0.018	0.06	Rivera et al. (2011)
4.0869	0.0059	0.15	28.211	0.042	0.15	Niespolo et al. (2017)
4.0749	0.0027	0.07	28.129	0.019	0.07	Phillips et al. (2017)
$R_{[FCTs/Mes4]}$[2]						
4.1780	0.0063	0.15	28.207	0.043	0.15	Kuiper et al. (2008)
4.1736	0.0025	0.06	28.274	0.096	0.34	Niespolo et al. (2017)

[1] $R_{FCTs/A1Ts} = [^{40}Ar^*/^{39}Ar]_{FCTs}/[^{40}Ar^*/^{39}Ar]_{A1Ts}$.
[2] $R_{FCTs/Mes4Ts} = [^{40}Ar^*/^{39}Ar]_{FCTs}/[^{40}Ar^*/^{39}Ar]_{Mes4Ts}$.

Here, we re-evaluate the astronomical calibration of the Fish Canyon Tuff sanidine (FCTs) in relation to sanidine from the astronomically tuned A1 Tephra (Faneromeni section, Crete; Kuiper et al., 2004; Rivera et al., 2011) and Mes4 tuff (Messâdit section, Morocco; Kuiper et al., 2008; Niespolo et al., 2017). To facilitate inter-laboratory comparisons that are independent of reference mineral ages and decay constants, we calculate R-values (see Renne et al., 1998) for FCTs relative to A1Ts and Mes4Ts, where:

$$R_{A1Ts}^{FCTs} = \frac{(e^{\lambda t_{FCTs}} - 1)}{(e^{\lambda t_{A1Ts}} - 1)} = \frac{\left(^{40}Ar^*/^{39}Ar_K\right)_{FCTs}}{\left(^{40}Ar^*/^{39}Ar_K\right)_{A1Ts}}$$

and

$$R_{Mes4Ts}^{FCTs} = \frac{(e^{\lambda t_{FCTs}} - 1)}{(e^{\lambda t_{Mes4Ts}} - 1)} = \frac{\left(^{40}Ar^*/^{39}Ar_K\right)_{FCTs}}{\left(^{40}Ar^*/^{39}Ar_K\right)_{Mes4Ts}}$$

Our analyses yield R-value that are consistent with most previous studies and permit the calculation of a revised, high precision age for the Fish Canyon Tuff sanidine reference mineral. In turn the new FCTs age allows calculation of revised ages for two other key reference minerals, Alder Creek Rhyolite sanidine (ACRs) and Mount Dromedary biotite (MD2b).

2. Samples

2.1. Faneromeni A1 tephra sanidine, Crete (A1Ts)

The A1 dacite-rhyolite tephra is an ~3 cm thick unit within the upper Faneromeni deep marine sedimentary sequence in Crete (Hilgen et al., 1997; Kuiper et al., 2004; Rivera et al., 2011). The A1T sanidine phenocrysts used in this study derive from the same sample analysed by Kuiper et al. (2004), Rivera et al. (2011) and Phillips et al. (2017). Astronomical tuning of the Faneromeni section produced an age of 6.941 ± 0.005 Ma for the A1 ash layer (Hilgen et al., 1997; Kuiper et al., 2004), revised to 6.943 ± 0.005 Ma (2σ) by Rivera et al. (2011).

2.2. Messâdit Mes4 tuff sanidine, Morocco (Mes4Ts)

The ~5 m thick Mes4 ignimbrite is one of several tephra units interbedded with marine sediments in the Messâdit section of the Melilla Basin, Morocco (Kuiper et al., 2008). The Mes4T sanidine phenocrysts used in this study are from the same sample analysed by Kuiper et al. (2008). Astronomical tuning of the Moroccan section gives an age of 6.791 ± 0.010 Ma (2σ) for the Mes4 tuff (Van Assen et al., 2006; Kuiper et al., 2008).

2.3. Fish Canyon tuff sanidine, Colorado (FCTs)

The well-known Fish Canyon Tuff (FCT) occurs in southern Colorado and forms part of the extensive San Juan Volcanic Field (e.g., Lipman et al., 1997). The tuff is described as a phenocryst-rich dacite/rhyolite tuff or a quartz-latite ignimbrite (Spell and McDougall, 2003) The FCT sample used in the current study derives from the same 'USGS' locality sampled by Spell and McDougall (2003).

3. Analytical methods

3.1. Sample preparation and irradiation

The A1T and Mes4T sanidine separates were prepared at the Vrije Universiteit, Amsterdam, using standard mineral separation methods (Kuiper et al., 2004; Kuiper et al., 2008). A1T sanidine grains ranged in size from 0.3–0.4 mm, with Mes4T sanidine grains being 0.8–1.0 mm in size. FCT sanidine crystals (0.3–0.4 mm) were prepared using methods described by Phillips and Matchan (2013). Transparent, inclusion-free sanidine crystals, with minimal adhering glass or groundmass material were selected for irradiation. All sanidine separates were ultrasonically cleaned with dilute (7%) hydrofluoric acid (~2 min) and washed thoroughly with de-ionised water and acetone.

To minimise neutron fluence gradients, small aliquots (<10 mg) of A1Ts + FCTs and Mes4Ts + FCTs sanidine grains were wrapped together in aluminium foil envelopes (~5 mm^2; ~2–3 grains deep). The packets were placed in the centre of silica glass tubes and irradiated in the U.S. Geological Survey's (USGS) TRIGA reactor or the CLICIT facility at the Oregon State University TRIGA (OSTR) reactor (Supplementary Table 1).

3.2. $^{40}Ar/^{39}Ar$ analytical procedures

$^{40}Ar/^{39}Ar$ analyses were undertaken in the Noble Gas laboratory at the University of Melbourne (UoM), using a multi-collector Thermo Fisher Scientific ARGUSVI mass spectrometer linked to a stainless steel gas extraction/purification line and a Photon Machines Fusions 10.6 CO_2 laser system (Phillips and Matchan, 2013). ^{40}Ar, ^{39}Ar and ^{37}Ar isotopes were measured on Faraday detectors (H1, AX, L2) with low noise 1×10^{13} Ω resistors. ^{38}Ar measurements were conducted on Faraday detector L1, with a low noise 1×10^{12} Ω resistor. A Compact Discrete Dynode (CDD) detector was utilized for ^{36}Ar measurements.

Air aliquots from an automated pipette system were analysed prior to sample analyses to monitor mass discrimination and Faraday/CCD detector bias relative to an atmospheric $^{40}Ar/^{36}Ar$ ratio of 298.56 ± 0.31 (Lee et al., 2006). Faraday detector bias was monitored via peak-jumping analyses on mass 40. Interference correction values for all irradiations, based on analyses of irradiated K-glass and CaF_2 samples in associated (longer) irradiations, are summarized in Supplementary Table 2. Contributions from $^{36}Ar_{Cl}$ were calculated using a $^{36}Cl/^{38}Cl$ production ratio of 257.8 ± 2.5 (Renne et al., 2008) and the $(^{36}Ar/^{38}Ar)_{Air}$ value of 5.3050 ± 0.0084 (Lee et al., 2006).

Following neutron irradiation, sanidine crystals were loaded into copper sample holders and placed into the stainless steel sample chamber with a ZnS cover slip. The extraction line was baked at ~100 °C until extraction line ^{40}Ar rate-of-rise levels had decreased to <1fA/min. Sample gas, introduced into the ARGUSVI mass spectrometer, was equilibrated for 20s, followed by multi-collection analysis of the five argon isotopes. Peak signals were regressed to time zero - the time of gas inlet into the mass spectrometer. Line blanks, measured between 1 and 3 sample analyses (typically <1.5 fA for ^{40}Ar; Supplementary Table 2), were subtracted from succeeding sample results.

3.3. $^{40}Ar/^{39}Ar$ data handling

In the current study, single crystal, total fusion, $^{40}Ar/^{39}Ar$ analyses were conducted on all A1T, Mes4T and FCT sanidine grains. The $^{40}Ar/^{39}Ar$ data were initially filtered to exclude analyses with low radiogenic $^{40}Ar^*$ (<80%), elevated Ca/K ratios (>0.5) or high associated blanks (> 2fA) (Supplementary Table 2). Following previous studies (Rivera et al., 2011; Niespolo et al., 2017), the data were then filtered using a normalized median absolute deviation (nMAD) value >3 (Powell et al., 2020). To evaluate the robustness of this statistical approach, we also used nMAD >2.5 and > 4 filters, and calculated robust Tukey Biweight mean values (Hoaglin et al., 1983; Ludwig, 2012) (Table 2).

R-values for FCTs relative to A1Ts and Mes4Ts were determined from weighted mean $^{40}Ar/^{39}Ar$ fusion results using the above methods (Table 2). As $^{39}Ar_K$ recoil loss data (e.g. Hall, 2013) are unavailable for A1Ts and Mes4Ts, we assumed similar values to FCTs (~0.18%; Hall, 2013), and no impact on R-values. FCTs ages were calculated relative to the astronomical ages for A1Ts (Rivera et al., 2011) and Mes4Ts (Kuiper et al., 2008), the atmospheric argon composition of Lee et al. (2006), and the decay constants recommended by Min et al. (2000). Note that

Table 2
Weighted mean R-values and $^{40}Ar^*/^{39}Ar$ ages for FCT, A1T and Mes4 sanidine fusion analyses from irradiations in this study.

Irradiation no.	Sample	No. grains	Wtd. mean $^{40}Ar^*/^{39}Ar$ (NMAD >2.5)	±2σ	Wtd. mean $^{40}Ar^*/^{39}Ar$ (NMAD >3)	±2σ	Wtd. mean $^{40}Ar^*/^{39}Ar$ (NMAD >4)	±2σ	Wtd. mean $^{40}Ar^*/^{39}Ar$ (Tukey)	±2σ	R-value (nMAD >2.5)	±2σ	R-value (nMAD >3)	±2σ	R-value (nMAD >4)	±2σ	R-value (Tukey)	±2σ
UM#75	FCTs	18	5.6693	0.0016	5.6693	0.0016	5.6693	0.0016	5.6692	0.0017	4.0833	0.0037	4.0857	0.0037	4.0857	0.0037	4.0838	0.0043
	A1Ts	15	1.3884	0.0012	1.3876	0.0012	1.3876	0.0012	1.3882	0.0014								
UM#82	FCTs	17	11.2191	0.0027	11.2191	0.0025	11.2202	0.0039	11.2198	0.0042	4.0789	0.0025	4.0804	0.0027	4.0808	0.0030	4.0802	0.0032
	A1Ts	26	2.7505	0.0015	2.7495	0.0017	2.7495	0.0018	2.7498	0.0019								
UM#85	FCTs	16	14.2941	0.0058	14.2941	0.0058	14.2909	0.0079	14.2932	0.0087	4.0812	0.0034	4.0812	0.0034	4.0803	0.0037	4.0809	0.0043
	A1Ts	21	3.5024	0.0026	3.5024	0.0026	3.5024	0.0026	3.5025	0.0030								
UM#87	FCTs	14	11.2311	0.0044	11.2311	0.0044	11.2311	0.0044	11.2309	0.0057	4.0806	0.0039	4.0806	0.0039	4.0806	0.0039	4.0841	0.0080
	A1Ts	11	2.7523	0.0024	2.7523	0.0024	2.7523	0.0024	2.7499	0.0053								
Mean (n = 4)											4.0806	0.0016	4.0817	0.0017	4.0818	0.0018	4.0815	0.0021
FCTs Age (Ma)											28.168	0.011	28.175	0.012	28.176	0.012	28.174	0.015
UM#89	FCTs	15	11.1930	0.0040	11.1930	0.0040	11.1930	0.0040	11.1939	0.0058	4.1732	0.0019	4.1727	0.0019	4.1728	0.0020	4.1730	0.0026
	Mes4	20	2.68211	0.00074	2.68242	0.00080	2.68242	0.00080	2.68249	0.00094								
UM#92	FCTs	12	9.2721	0.0045	9.2721	0.0045	9.2721	0.0045	9.2720	0.0047	4.1745	0.0024	4.1745	0.0024	4.1750	0.0025	4.1745	0.0026
	Mes4	20	2.22115	0.00067	2.22115	0.00067	2.22084	0.00078	2.22108	0.00083								
Mean (n = 2)											4.1737	0.0015	4.1734	0.0015	4.1735	0.0015	4.1737	0.0018
FCTs Age (Ma)											28.178	0.010	28.176	0.010	28.177	0.010	28.178	0.012
R(A1Ts/Mes4)											0.97769	0.00052	0.97803	0.00054	0.97803	0.00056	0.97791	0.00066

the choice of decay constants (e.g., Steiger and Jäger, 1977; Renne et al., 2010, 2011; Carter et al., 2020) has negligible impact on calculated R-values and ages. Unless otherwise stated, uncertainties associated with R-values and ages are reported at the 2σ level and exclude uncertainties in the ages of A1Ts and Mes4Ts and decay constants. Final FCTs ages are reported with both internal and external uncertainties (i.e. including uncertainties in the ages of A1Ts and Mes4Ts).

4. Results

Single crystal laser fusion analyses were conducted on A1T, Mes4T and FCT sanidine aliquots across multiple irradiation batches (Supplementary Table 2). Weighted mean $^{40}Ar^*/^{39}Ar$ and R-values for each sample batch are tabulated in Table 2. $^{40}Ar^*/^{39}Ar$ and Ca/K ratios are compared in Figs. 1 and 2.

Calculated Ca/K ratios for FCTs range from 0.01 to 0.04, with most values between 0.01 and 0.02 (Figs. 1, 2). Aside from two feldspar crystals (UM#85) with elevated ratios (Ca/K > 4.3; Supplementary Table 2), A1Ts Ca/K values are broadly similar, ranging from 0.005 to 0.045, although most plot between 0.01 and 0.03 (Fig. 1). Mes4Ts crystals exhibit a narrow range of Ca/K ratios from 0.028 to 0.036 (Fig. 2). The variations in Ca/K ratios are consistent with fractional crystallisation processes and the lack of any clear correlation with $^{40}Ar^*/^{39}Ar$ values suggests the absence of obvious megacrysts, xenocrysts or antecrysts in the sample aliquots.

Weighted mean $^{40}Ar^*/^{39}Ar$ and R-values are relatively insensitive to the statistical filter used (Table 2; Figs. 1, 2). For consistency with previous studies (e.g. Rivera et al., 2011; Niespolo et al. (2017), we compare results based on the nMAD >3 filter. Mean $^{40}Ar^*/^{39}Ar$ ratios for most sample aliquots are characterised by MSWD values >1 (up to 2.6; Figs. 1, 2), analogous to the observations in Phillips et al. (2017). Possible causes of the excess dispersion could include analytical aberrations (e.g. anomalous blanks), variable neutron fluence gradients and/or geological factors (e.g. inherited or excess argon). Reported neutron fluence gradients for the CLICIT facility average ~ 0.05–0.1% mm^{-1} (Rutte et al., 2018) and could account for most of the observed dispersion about the mean (~0.1%), although we cannot negate other analytical and geological factors operating at this level.

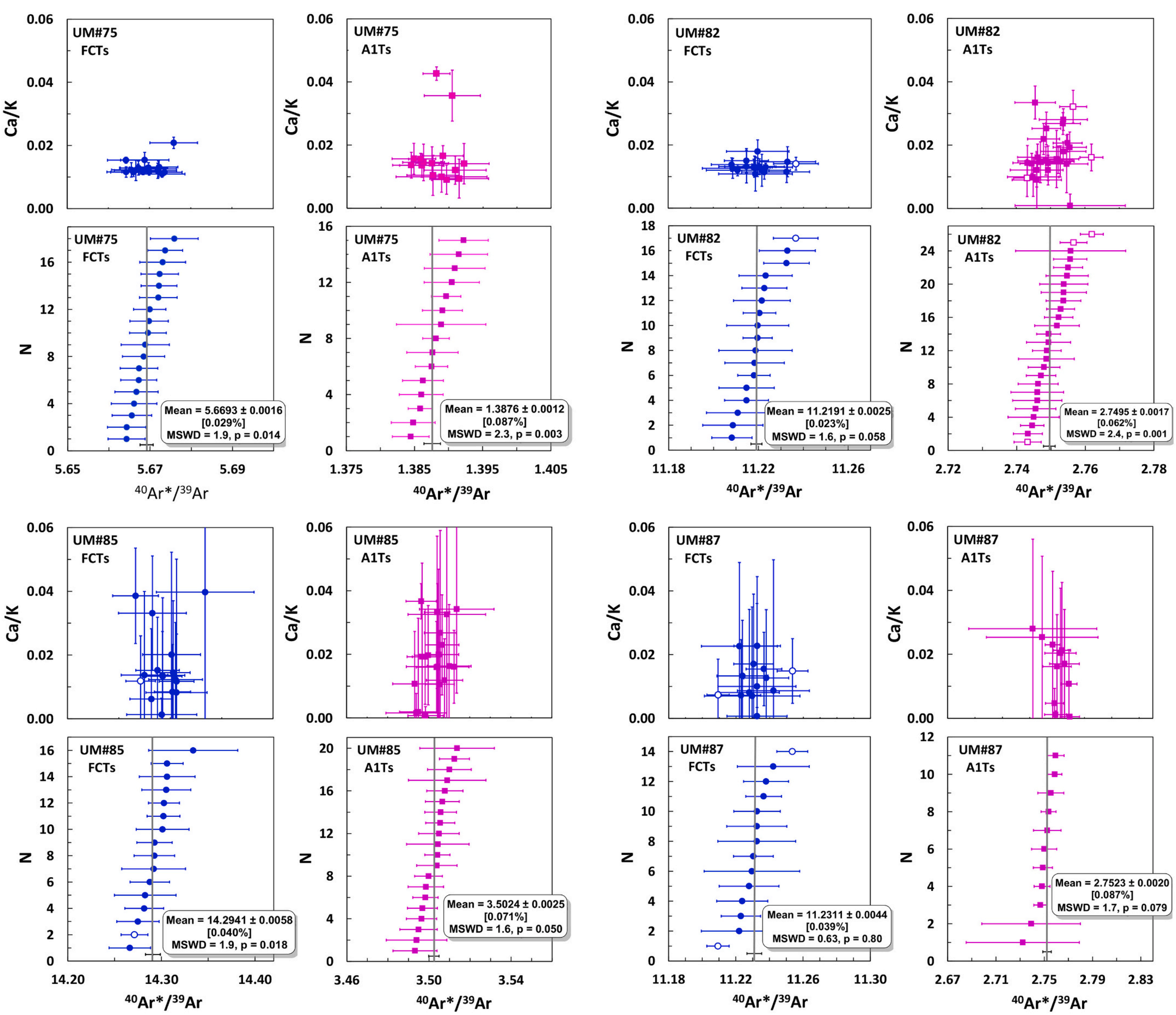

Fig. 1. $^{40}Ar/^{39}Ar^*$ and Ca/K ratios for Fish Canyon Tuff sanidine versus A1 Tuff sanidine. Weighted mean $^{40}Ar/^{39}Ar^*$ values calculated using Isoplot (Ludwig, 2012). Open symbols represent analyses excluded from the weighted mean $^{40}Ar/^{39}Ar^*$ ratio based on nMAD >3 filtering.

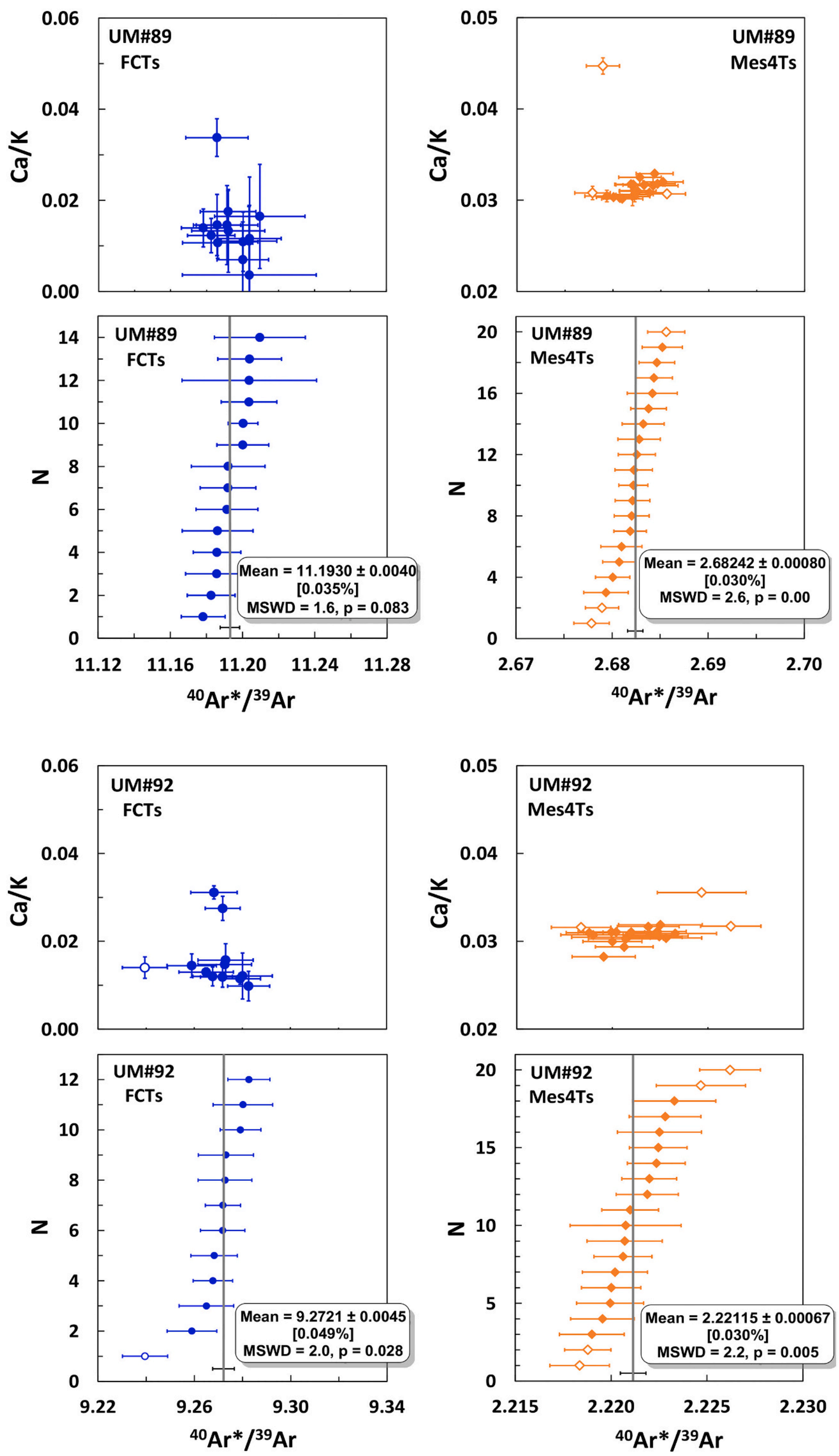

Fig. 2. $^{40}Ar/^{39}Ar^*$ and Ca/K ratios for Fish Canyon Tuff sanidine versus Mes4 Tuff sanidine. Weighted mean $^{40}Ar/^{39}Ar^*$ values calculated using Isoplot (Ludwig, 2012). Open symbols represent analyses excluded from the weighted mean $^{40}Ar/^{39}Ar^*$ ratio based on nMAD >3 filtering.

R_{A1Ts}^{FCTs}-values, calculated for co-irradiated A1Ts and FCTs aliquots, are analogous across the four irradiation batches (UM#75, UM#82, UM#85, UM#87), and range from 4.0857 ± 0.0037 (0.092%; 2σ) to 4.0804 ± 0.0027 (0.066%; 2σ), giving a weighted mean value of 4.0817 ± 0.0017 (0.041%; 2σ). This equates to FCTs ages ranging from 28.202 ± 0.026 Ma to 28.166 ± 0.020 Ma, giving a mean value of 28.175 ± 0.012 Ma, relative to an astronomically tuned age of 6.943 ± 0.005 Ma for the A1 tuff (Rivera et al., 2011). For comparison, the robust Tukey Biweight mean R_{A1Ts}^{FCTs}-value is 4.0815 ± 0.0021, yielding an age of 28.174 ± 0.015 Ma (Table 2).

$^{40}Ar/^{39}Ar$ data from irradiation batches UM#89 and UM#92 yielded indistinguishable R_{Mes4Ts}^{FCTs}-values for co-irradiated Mes4T and FCT sanidine aliquots, of 4.1727 ± 0.0019 (0.046%; 2σ) and 4.1745 ± 0.0024 (0.057%; 2σ), yielding a mean value of 4.1734 ± 0.0015 (0.036%; 2σ). This equates to FCTs ages of 28.172 ± 0.013 Ma and 28.183 ± 0.016 Ma and a mean value of 28.176 ± 0.010 Ma, relative to an age of 6.791 ± 0.005 Ma for the Mes4 tuff (Kuiper et al., 2008). These results are indistinguishable from the Tukey Biweight mean R_{A1Ts}^{FCTs}-

value of 4.1737 ± 0.0018 and FCTs age of 28.178 ± 0.012 Ma (Table 2).

5. Discussion

R-values provide a useful approach for comparing $^{40}Ar/^{39}Ar$ results from multiple irradiations and different laboratories. In this section, we first compare our results with previous astrological inter-calibration studies, before evaluating the optimal astronomically calibrated age for FCTs and other $^{40}Ar/^{39}Ar$ reference minerals.

5.1. Comparison with previous astrochronological results

R_{A1Ts}^{FCTs}-values determined in the current study are compared with those from previous studies in Fig. 3. The average R_{A1Ts}^{FCTs}-value (4.0817 ± 0.0017) determined from this study is within uncertainty of previous R-values measured by Kuiper et al. (2004), Rivera et al. (2011) and Niespolo et al. (2017) (Fig. 3). The improved precision of the current results is largely attributable to the higher precision capability of the ARGUSVI mass spectrometer system, with uncertainties on individual FCTs $^{40}Ar^{*}/^{39}Ar$ ratios typically <0.05% (1σ), compared to uncertainties >0.2% recorded in earlier studies (Rivera et al., 2011; Niespolo et al., 2017).

The current R_{A1Ts}^{FCTs}-value is distinct (~0.15% higher) from that reported by Phillips et al. (2017); reasons for this discordance are unclear. Possible explanations include undetected fluctuations in analytical conditions, minor extraneous argon in the larger A1Ts crystals used in the earlier study and/or variations in neutron fluence, possibly exacerbated by separation of co-irradiated A1Ts and FCTs crystals.

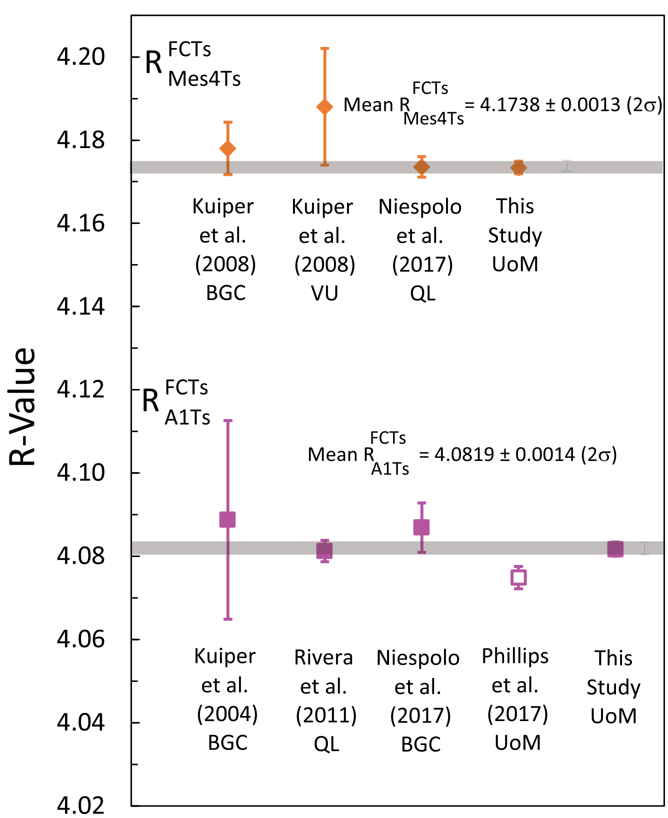

Fig. 3. R_{A1Ts}^{FCTs} and R_{Mes4Ts}^{FCTs} values from previous work and the current study. Filled symbols indicate R-values included in the inter-laboratory weighted mean calculations; open symbols indicate R-values excluded from these calculations (see text for details). Horizontal grey bars represent 2σ uncertainties in weighted mean R-values. BGC = Berkeley Geochronology Centre; VU = Vrije Universiteit; QL = Quaternary Dating Laboratory, Roskilde University; UoM = University of Melbourne.

Given neutron fluence gradients of ~0.05–0.1% mm^{-1} (Rutte et al., 2018), separation by ~2–3 mm would be sufficient to account for the above difference. Instrumental bias is considered unlikely, because R_{FCTs}^{ACRs}-values (where ACRs is the well-known Alder Creek Rhyolite sanidine reference mineral) reported by Phillips et al. (2017) are indistinguishable from those reported by Niespolo et al. (2017) and Rivera et al. (2013).

The mean R_{Mes4Ts}^{FCTs}-value (4.1734 ± 0.0015) from this study is within uncertainty (2σ) of the values determined by Kuiper et al. (2008; at both the Berkeley Geochronology Centre and Vrije Universiteit laboratories) and Niespolo et al. (2017). This comparison is maintained regardless of whether sanidine analyses from all Messâdit tuffs are included in the comparison (Fig. 1).

In combination, the new R_{A1Ts}^{FCTs}- and R_{Mes4Ts}^{FCTs}-values indicate good agreement between the four $^{40}Ar/^{39}Ar$ laboratories for which relevant data are available, noting that the earlier data from Kuiper et al. (2004, 2008) were not determined using modern multi-collector mass spectrometers. These results give weighted mean, inter-laboratory R_{A1Ts}^{FCTs}- and R_{Mes4Ts}^{FCTs}-values of 4.0819 ± 0.0014 (0.034%) and 4.1738 ± 0.0013 (0.030%), respectively.

5.2. Astronomically calibrated age for FCTs

The above R-values can be used to calculate revised astronomically calibrated ages for FCTs (Fig. 2). Relative to ages of 6.943 ± 0.005 Ma for A1Ts (Rivera et al., 2011) and 6.791 ± 0.010 Ma for the Mes4 tuff (Kuiper et al., 2008), the current data equate to FCTs ages of 28.175 ± 0.012 Ma (2σ; ±0.023 Ma including the uncertainty in the age of A1Ts) and 28.176 ± 0.010 Ma (2σ; ±0.042 Ma including the uncertainty in the age of Mes4Ts) (Fig. 2).

The improved agreement in measured R-values (R_{A1Ts}^{FCTs}, R_{Mes4Ts}^{FCTs}) across multiple irradiations and $^{40}Ar/^{39}Ar$ laboratories also permits determination of a revised astronomically calibrated, inter-laboratory age for FCTs (Fig. 4). We calculate an inter-laboratory weighted mean FCTs age of 28.176 ± 0.010 (±0.023) Ma, including external uncertainties) relative to the age of A1Ts, and an age of 28.179 ± 0.009 Ma (±0.042 Ma, including external uncertainties) relative to the astronomical age of Mes4Ts. Consideration of all Messâdit sanidine results reported by Kuiper et al. (2008) yields an analogous mean age of 28.181 ± 0.020 Ma (±0.046 Ma) (Fig. 4).

Although the above astronomically calibrated FCTs ages are indistinguishable, the astronomical age assigned to A1Ts is more precise than that of Mes4Ts. Consequently, we recommend that the interlaboratory, astronomically calibrated mean value of 28.176 ± 0.010 (±0.023) Ma be adopted as the age of the FCTs fluence monitor.

The above age is within uncertainty of the $^{206}Pb/^{238}U$ age of 28.196 ± 0.038 Ma reported for FCT zircons by Wotzlaw et al. (2013), but numerically distinct from FCTs ages of 28.10 Ma (Westerhold et al., 2015) and 28.150 Ma (Channell et al., 2020) inferred from recent deep-sea core data, although no uncertainties are reported. Using the $^{40}Ar/^{39}Ar$ data documented for Ash-17 by Storey et al. (2007) and an uncertainty of 50 ka in astronomical tuning (Westerhold et al., 2015), we calculate an FCTs age of 28.10 ± 0.04 Ma (2σ; internal uncertainties). The FCTs age of 28.150 Ma reported by Channell et al. (2020) is based on the minimum offset between the astronomical and $^{40}Ar/^{39}Ar$ ages for 16 geomagnetic excursions with no uncertainty assigned. Both these ages remain distinct from our preferred age of 28.176 ± 0.011 Ma for FCTs. Clearly, further studies of astronomically tuned ODP sections containing ash-beds amenable to $^{40}Ar/^{39}Ar$ dating are needed.

5.3. Revised astronomically calibrated ages for Alder Creek Rhyolite sanidine (ACRs) and Mount Dromedary biotite (MD-2)

In addition to FCTs, other widely utilized reference minerals include the ca.1.18 Ma Alder Creek Rhyolite sanidine (ACRs) (e.g., Turrin et al.,

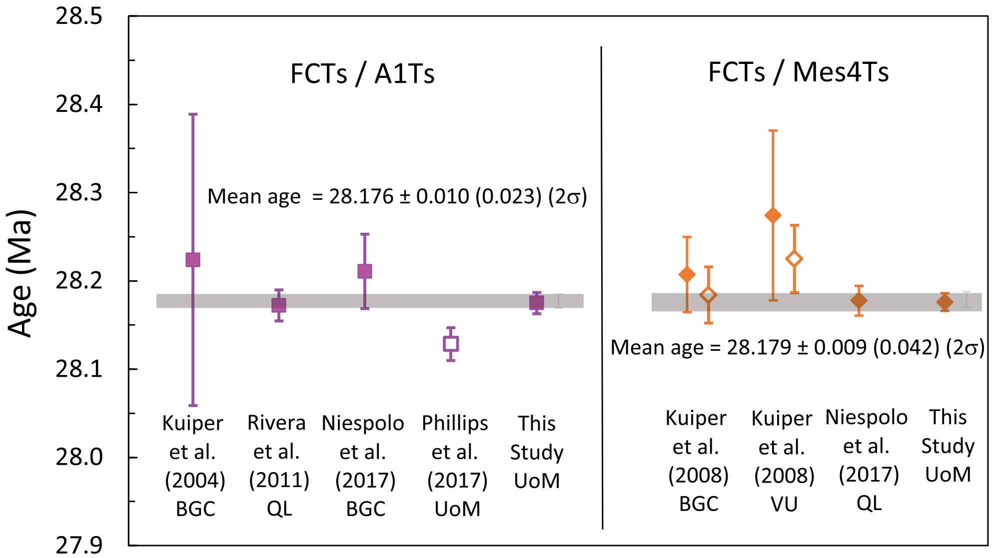

Fig. 4. FCT sanidine $^{40}Ar/^{39}Ar$ ages from the current study compared with results from previous work. FCTs ages are calculated relative to the astronomically tuned ages for A1Ts (Kuiper et al., 2004; Rivera et al., 2011) and Mes4Ts (Kuiper et al., 2008). Filled symbols indicate age values included in the inter-laboratory weighted mean calculations. Open symbols indicate values excluded from these calculations (see text for details). Horizontal grey bars represent 2σ uncertainties in weighted mean ages. Values in brackets include uncertainties in the ages of A1Ts or Mes4Ts. Abbreviations as per Fig. 1.

1994) and the ca.99.1 Ma Mount Dromedary biotite (GA-1550 and MD-2) (e.g., McDougall and Wellman, 2011; Phillips et al., 2017).

The Alder Creek Rhyolite is located on Cobb Mountain, Sonoma County, California and forms part of the Clear Lake Volcanic Field (e.g., Mankinen et al., 1978; Turrin et al., 1994). The ACR is characterised by transitional geomagnetic polarity and is considered to record the geomagnetic reversal as the top of the Cobb Mountain Normal Polarity subchron (e.g., Singer, 2014). Previous attempts to date the ACR are summarized in Schaen et al. (2021). Based on the mean R_{FCTs}^{ACRs}-value of 0.041692 ± 0.000024 (0.058%) reported by Phillips et al. (2017, 2020), and assuming negligible relative $^{39}Ar_K$ recoil loss, we calculate an age of 1.18342 ± 0.00069 Ma (±0.0090 Ma, including external uncertainties) for the Alder Creek Rhyolite, compared to an FCTs age of 28.176 ± 010 Ma. The above R_{FCTs}^{ACRs}-value is within uncertainty of the interlaboratory mean of 0.041715 ± 0.000029 (0.069%) reported by Schaen et al. (2021), noting that this value includes the Phillips et al. (2017, 2020) data. This equates to an ACRs age of 1.18403 ± 0.00082 (±0.011) Ma (relative to an FCTs age of 28.176 ± 0.010 Ma).

The Mount Dromedary igneous complex is located in New South Wales, Australia (e.g., Boesen and Joplin, 1972; Smith et al., 1988). The GA-1550 (see McDougall and Wellman, 2011) and MD-2 (Phillips et al., 2017) biotite samples were collected from the same outer monzonite unit of the complex. Previous geochronological studies of the Mount Dromedary complex are summarized by Phillips et al. (2017). Using the R_{FCTs}^{MD2b}-value of 3.5948 ± 0.0028 (2σ) from the latter study, we calculate a revised astronomically calibrated age for MD-2 biotite (MD2b) of 99.323 ± 0.077 Ma (±0.33 Ma, including external uncertainties). This equates to a recoil affected age of 99.20 ± 0.01 (±0.38) Ma, using $^{39}Ar_K$ recoil loss levels reported by Hall (2013). Both ages are within uncertainty of the $^{238}U/^{206}Pb$ zircon age of 99.12 ± 0.14 Ma obtained by Schoene et al. (2006).

6. Conclusions

$^{40}Ar/^{39}Ar$ analyses of Fish Canyon Tuff sanidine (FCTs) crystals, co-irradiated with A1 Tephra sanidine (A1Ts) and Mes4 Tuff sanidine (Mes4Ts) yield a mean R_{A1Ts}^{FCTs}-value of 4.0817 ± 0.0017 and a mean R_{Mes4Ts}^{FCTs}-value of 4.1734 ± 0.0015, equating to FCTs ages of 28.175 ± 0.012 (±0.023) Ma and 28.176 ± 0.010 (±0.042) Ma, respectively, relative to astronomically tuned ages for A1Ts (Rivera et al., 2011) and Mes4Ts (Kuiper et al., 2008). These R-values and ages are consistent with most previously reported FCTs ages calibrated against A1Ts and Mes4Ts, giving mean inter-laboratory ages of 28.176 ± 0.010 (± 0.023) Ma and 28.179 ± 0.009 (±0.042) Ma, respectively. It is recommended that the former age be adopted as the astronomical age for FCTs. Using previous R-values for the Alder Creek Rhyolite sanidine (ACRs) and Mount Dromedary biotite (MD2b) reference minerals co-irradiated with FCTs, we calculate revised astronomically calibrated ages of 1.18342 ± 0.00069 (±0.009) Ma and 99.323 ± 0.077 Ma (±0.33) Ma, respectively, with the latter corrected to 99.20 ± 0.01 (±0.38) Ma to account for recoil loss of $^{39}Ar_K$.

Declaration of Competing Interest

None.

Acknowledgements

This study is supported by AuScope and an Australian Research Council Discovery grant (DP180101412) to DP and EM. S. Szczepanski is thanked for technical assistance in the University of Melbourne $^{40}Ar/^{39}Ar$ laboratory. The manuscript has benefitted from formal reviews by two anonymous reviewers and the editor, B. Kamber.

Appendix A. Supplementary data

Supplementary data to this article can be found online at https://doi.org/10.1016/j.chemgeo.2022.120815.

References

Boesen, R.S., Joplin, G.A., 1972. The form of the intrusive complex at Mount Dromedary, New South Wales. J. Geol. Soc. Aust. 19, 345–349.

Carter, J., Ickert, R.B., Mark, D.F., Tremblay, M.M., Cresswell, A.J., Sanderson, D.C.W., 2020. Production of ^{40}Ar by an overlooked mode of ^{40}K decay with implications for K-Ar geochronology. Geochron. 2, 355–365.

Cebula, G.T., Kunk, M.J., Mehnert, H.H., Naeser, C.W., Obradovich, J.D., Sutter, J.F., 1986. The fish Canyon Tuff, a potential standard for the ^{40}Ar–^{39}Ar and fission-track dating methods. Terra Cognita 6, 139–140.

Channell, J.E.T., Singer, B.S., Jicha, B.R., 2020. Timing of Quaternary geomagnetic reversals and excursions in volcanic and sedimentary archives. Quat. Sci. Rev. 228, 106114.

Ganerød, M., Chew, D.M., Smethurst, M.A., Troll, V.R., Corfu, F., Meade, F., Prestvik, T., 2011. Geochronology of the Tardee Rhyolite complex, Northern Ireland: Implications of fission track studies, the North Atlantic Igneous Province and the age of the fish Canyon sanidine standard. Chem. Geol. 286, 222–228.

Hall, C.M., 2013. Direct measurement of recoil effects on $^{40}Ar/^{39}Ar$ standards. In Advances in $^{40}Ar/^{39}Ar$ Dating: from Archaeology to Planetary Sciences (eds. F. Jourdan, D.F. Mark and C. Verati); Geol. Soc. Lond. Spec. Publ, p. 378.

Hilgen, F.J., Krijgsman, W., Wijbrans, J.R., 1997. Direct comparison of astronomical and $^{40}Ar/^{39}Ar$ ages of ash beds: potential implications for the age of mineral dating standards. Geophys. Res. Lett. 24, 2043–2046.

Hoaglin, D.C., Mosteller, F., Tukey, J.W., 1983. Understanding Robust and Exploratory Data Analysis. John Wiley and Sons, pp. 345–349.

Knox, R.W.O.B., 1984. Nanoplankton zonation and the Palaeocene/Eocene boundary beds of NW Europe: an indirect correlation by means of volcanic ash layers. J. Geol. Soc. 141, 993–999.

Kuiper, K.F., Hilgen, F.J., Steenbrink, J., Wijbrans, J.R., 2004. $^{40}Ar/^{39}Ar$ ages of tephras intercalated in astronomically tuned Neogene sedimentary sequences in the eastern Mediterranean. Earth Planet. Sci. Lett. 222, 583–597.

Kuiper, K.F., Deino, A., Hilgen, F.J., Krijgsman, W., Renne, P.R., Wijbrans, J.R., 2008. Synchronizing rock clocks of Earth history. Science 320, 500–504.

Lanphere, M.A., Baadsgaard, H., 2001. Precise K–Ar, $^{40}Ar/^{39}Ar$, Rb–Sr, U/Pb mineral ages from the 27.5 Ma Fish Canyon Tuff reference standard. Chem. Geol. 175, 653–671.

Lee, J.-Y., Marti, K., Severinghaus, J.P., Kawamura, K., Yoo, H.-S., Lee, J.B., Kim, J.S., 2006. A redetermination of the isotopic abundances of atmospheric Ar. Geochim. Cosmochim. Acta 70, 4507–4512.

Lipman, P.W., Dungan, M.A., Bachmann, O., 1997. Comagmatic granophyric granite in the fish Canyon Tuff, Colorado: implications for magma-chamber processes during a large ash-flow eruption. Geology 25, 915–918.

Ludwig, K.R., 2012. User's Manual for Isoplot 3.75. A Geochronological Toolkit for Microsoft Excel: Spec. Publ. No. 5. Berkeley Geochronology Center, Berkeley, California, p. 75.

Mankinen, E.A., Donnelly, J.M., GrommeÅL, C.S., 1978. Geomagnetic polarity event recorded at 1.1 m.y. B.P. on Cobb Mountain, Clear Lake Volcanic field. Calif. Geol. 6, 653–656.

McDougall, I., Wellman, P., 2011. Calibration of GA1550 biotite standard for K/Ar and $^{40}Ar/^{39}Ar$ dating. Chem. Geol. 280, 19–25.

Min, K.W., Mundil, R., Renne, P.R., Ludwig, K.R., 2000. A test for systematic errors in $^{40}Ar/^{39}Ar$ geochronology through comparison with U/Pb analysis of a 1.1-Ga rhyolite. Geochim. Cosmochim. Acta 64, 73–98.

Niespolo, E.M., Rutte, D., Deino, A.L., Renne, P.R., 2017. Intercalibration and age of the Alder Creek sanidine $^{40}Ar/^{39}Ar$ standard. Quat. Geochronol. 39, 205–213.

Phillips, D., Matchan, E.L., 2013. Ultra-high precision $^{40}Ar/^{39}Ar$ ages for fish canyon tuff and Alder Creek Rhyolite sanidine: new dating standards required? Geochim. Cosmochim. Acta 121, 229–239.

Phillips, D., Matchan, E.L., 2020. Corrigendum to "Ultra-high precision $^{40}Ar/^{39}Ar$ ages for fish canyon tuff and Alder Creek Rhyolite sanidine: new dating standards required?" [Geochim. Cosmochim. Acta 121 (2013) 229-239]. Geochim. Cosmochim. Acta 273, 403–405.

Phillips, D., Matchan, E.L., Honda, M., Kuiper, K.F., 2017. Astronomical calibration of $^{40}Ar/^{39}Ar$ reference minerals using high-precision, multi-collector (ARGUSVI) mass spectrometry. Geochim. Cosmochim. Acta 196, 351–369.

Phillips, D., Matchan, E.L., Honda, M., Kuiper, K.F., 2020. Corrigendum to "Astronomical calibration of $^{40}Ar/^{39}Ar$ reference minerals using high-precision, multi-collector (ARGUSVI) mass spectrometry". [Geochim. Cosmochim. Acta 196 (2017) 351-369]. Geochim. Cosmochim. Acta 273, 406–410.

Powell, R., Green, E.C.R., Marillo Sialer, E., Woodhead, J., 2020. Robust isochron calculation. Geochron. 2, 325–342.

Renne, P.R., Swisher, C.C., Deino, A.L., Karner, D.B., Owens, T.L., DePaolo, D.J., 1998. Intercalibration of standards, absolute ages and uncertainties in $^{40}Ar/^{39}Ar$ dating. Chem. Geol. 145, 117–152.

Renne, P.R., Sharp, Z.D., Heizler, M.T., 2008. Cl-derived argon isotope production in the CLICIT facility of OSTR reactor and the effects of the Cl-correction in $^{40}Ar/^{39}Ar$ geochronology. Chem. Geol. 255, 463–466.

Renne, P.R., Mundil, R., Balco, G., Min, K., Ludwig, K.R., 2010. Joint determination of ^{40}K decay constants and $^{40}Ar^*/^{40}K$ for the fish Canyon sanidine standard, and improved accuracy for $^{40}Ar/^{39}Ar$ geochronology. Geochim. Cosmochim. Acta 74, 5349–5367.

Renne, P.R., Balco, G., Ludwig, K.R., Mundil, R., Min, K., 2011. Response to the comment by W.H. Schwarz et al. on "Joint determination of ^{40}K decay constants and $^{40}Ar^*/^{40}K$ for the fish Canyon sanidine standard, and improved accuracy for $^{40}Ar/^{39}Ar$ geochronology" by P.R. Renne et al., 2010. Geochim. Cosmochim. Acta 75, 5097–5100.

Rivera, T.A., Storey, M., Zeeden, C., Hilgen, F.J., Kuiper, K., 2011. A refined astronomically calibrated $^{40}Ar/^{39}Ar$ age for fish Canyon sanidine. Earth Planet. Sci. Lett. 311, 420–426.

Rivera, T.A., Storey, M., Schmitz, M.D., Crowley, J.L., 2013. Age intercalibration of $^{40}Ar/^{39}Ar$ sanidine and chemically distinct U/Pb zircon populations from the Alder Creek Rhyolite Quaternary geochronology standard. Chem. Geol. 345, 87–98.

Rutte, D., Becker, T.A., Deino, A.L., Reese, S.R., Renne, P.R., Schickler, R.A., 2018. The new CLOCIT irradiation facility for $^{40}Ar/^{39}Ar$ geochronology: characterization, comparison with CLICIT and implications for high-precision geochronology. Geostand. Geoanal. Res. 42 (3), 301–307.

Schaen, A.J., Jicha, B.R., Hodges, K.V., Vermeesch, P., Stelten, M.E., Mercer, C.M., Phillips, D., Rivera, T.A., Jourdan, F., Matchan, E.L., Hemming, S.R., Morgan, L.E., Kelley, S.P., Cassata, W.S., Heizler, M.T., Vasconcelos, P.M., Benowitz, J.A., Koppers, A.A.P., Mark, D.F., Niespolo, E.M., Sprain, C.J., Hames, W.E., Kuiper, K.F., Turrin, B.D., Renne, P.R., Ross, J., Nomade, S., Guillou, H., Webb, L.E., Cohen, B.A., Calvert, A.T., Joyce, N., Ganerød, M., Wijbrans, J., Ishizuka, O., He, H., Ramirez, A., Pfänder, J.A., Lopez-Martínez, M., Qiu, H., Singer, B.S., 2021. Interpreting and reporting $^{40}Ar/^{39}Ar$ geochronologic data. GSA Bull. 133 (3–4), 461–487.

Schoene, B., Crowley, J.L., Condon, D.J., Schmitz, M.D., Bowring, S.A., 2006. Reassessing the uranium decay constants for geochronology using ID-TIMS U–Pb data. Geochim. Cosmochim. Acta 70, 426–445.

Singer, B.S., 2014. A quaternary geomagnetic instability time scale. Quat. Geochronol. 21, 29–52.

Smith, I.E.M., White, A.J.R., Chappell, B.W., Eggleton, R.A., 1988. Fractionation in a zoned monzonite pluton: Mount Dromedary, southeastern Australia. Geol. Mag. 125, 273–284.

Spell, T.L., McDougall, I., 2003. Characterization and calibration of $^{40}Ar/^{39}Ar$ dating standards. Chem. Geol. 198, 189–211.

Steiger, R.H., Jäger, E., 1977. Subcommission on geochronology: convention on the use of decay constants in geo- and cosmochronology. Earth Planet. Sci. Lett. 36, 359–362.

Storey, M., Duncan, R.A., Swisher III, C.C., 2007. Paleocene-Eocene thermal Maximum and the opening of the Northeast Atlantic. Science 316, 587–589.

Turrin, B.D., Donnely-Nolan, J.M., Hearn, B.C., 1994. $^{40}Ar/^{39}Ar$ ages from the rhyolite of Alder Creek, California: age of the Cobb Mountain normal-polarity subchron revisited. Geology 22, 251–254.

Van Assen, E., Kuiper, K.F., Barhoun, N., Krijgsman, W., Sierro, F.J., 2006. Messinian astrochronology of the Melilla Basin: stepwise restriction of the Mediterranean–Atlantic connection through Morocco. Paleogeog. Paleoclimat. Paleoecol. 238, 15–31.

Westerhold, T., Röhl, U., Frederichs, S., Bohaty, S.M., Zachos, J.C., 2015. Astronomical calibration of the geological timescale: closing the middle Eocene gap. Clim. Past 11, 1181–1195.

Wotzlaw, J.-F., Schaltegger, U., Frick, D.A., Dungan, M.A., Gerdes, A., Gunther, D., 2013. Tracking the evolution of largevolume silicic magma reservoirs from assembly to supereruption. Geology 41 (8), 867–870.